Electron Paramagnetic Resonance Imaging of Rat Heart with Nitroxide and Polynitroxyl-Albumin†

Periannan Kuppusamy, Penghai Wang, and Jay L. Zweier*

Molecular and Cellular Biophysics Laboratories, Department of Medicine, Division of Cardiology, and EPR Center, Johns Hopkins Medical Institutions, 5501 Hopkins Bayview Circle, Baltimore, Maryland 21224

Murali C. Krishna and James B. Mitchell

Radiation Biology Branch, National Cancer Institute, Building 10-B3 B69, National Institutes of Health, Bethesda, Maryland 20892

Li Ma, Charles E. Trimble, and Carleton J. C. Hsia‡

SynZyme Technologies, Inc., One Technology Drive, Suite E-309, Irvine, California 92718

Received December 4, 1995; Revised Manuscript Received March 5, 1996⊗

ABSTRACT: Electron paramagnetic resonance (EPR)[1] imaging utilizing stable nitroxyl radicals is a promising technique for measuring free radical distribution, metabolism, and tissue oxygenation in organs and tissues [Kuppusamy, P., Chzhan, M., Vij, K., Shteynbuk, M., Lefer, D. J., Giannella, E., & Zweier, J. L. (1994) *Proc. Natl. Acad. Sci. U.S.A. 91*, 3388−3392]. However, the technique has been limited by the rapid reduction of nitroxide *in vivo* to its hydroxylamine derivative, a diamagnetic, EPR-inactive species. In this report a novel, polynitroxylated derivative of human serum albumin is shown to be capable of reoxidizing the hydroxylamine back to nitroxide *in vivo*. Polynitroxyl-albumin (PNA) is shown to be effective in maintaining the signal intensity of the nitroxide 4-hydroxy-2,2,6,6-tetramethylpiperidine-1-oxyl (TEMPOL or TPL) in the ischemic isolated rat heart, allowing the acquisition of high-resolution three-dimensional (3D) EPR images of the heart throughout a prolonged 2.5 h period of global cardiac ischemia. In serial transverse sections of the 3D image, TPL intensity maps of the heart showed cardiac structure with submillimeter resolution. TPL intensities in coronary arteries and myocardium showed that nitroxide concentration decreases with increasing distance from large blood vessels. These results demonstrate that EPR imaging *in vivo* is possible using nitroxides in conjunction with PNA. In addition to its utility in the emerging technology of EPR imaging, the greatly prolonged half-life of TPL observed in the presence of PNA may facilitate the therapeutic application of nitroxides in a variety of disease processes.

Stable nitroxyl radicals (nitroxides) have been used as probes of biophysical and biochemical properties, including membrane fluidity and molecular conformation (Martinez-Yamout & McConnell, 1994). In addition, nitroxides have been shown to function as mimics of the antioxidant enzymes superoxide dismutase (Krishna et al., 1992; Samuni et al., 1988; Voest et al., 1993) and catalase (Mehlhorn & Swanson, 1992; Reddan et al., 1993) and as potential agents of cytoprotection against damage by ionizing radiation (Hahn et al., 1994; Johnstone et al., 1995) and against postischemic reperfusion injury (Gelvan et al., 1991). Nitroxides are also potential contrast agents for magnetic resonance imaging (MRI)[1] (Brasch, 1983; Brasch et al., 1983; Chan et al., 1990; Eriksson et al., 1988; Swartz, 1987, 1989; Swartz et al., 1986). Because the electron paramagnetic resonance (EPR) signal of nitroxide reflects local oxygen concentration, and because nitroxides are reduced preferentially in hypoxic tissue to a diamagnetic (EPR-silent) hydroxylamine derivative, nitroxides can add metabolic information, in addition to the anatomic information provided by conventional MRI contrast agents (Brasch, 1983; Brasch et al., 1983; Chan et al., 1990; Eriksson et al., 1988; Swartz, 1987, 1989; Swartz et al., 1986). We have therefore developed instrumentation for EPR imaging, an emerging technology that shows great promise in medical research (Berliner, 1992; Berliner et al., 1987), particularly in the imaging of ischemic tissue (Zweier & Kuppusamy, 1988; Kuppusamy et al., 1994, 1995a−c). Nitroxides have recently been used to obtain three-dimensional (3D) EPR images of the isolated rat heart and the rabbit aorta, allowing tissue oxygen metabolism to be studied and the development of hypoxia visualized (Kuppusamy et al., 1994). However, high-resolution EPR imaging has been prevented by the rapid decay (half-life ∼3 min) of the nitroxide EPR signal in the ischemic heart. This decay is the result of reduction of nitroxide to hydroxylamine. The mechanism of reduction *in vivo* depends on several factors including the structure of the nitroxide, oxygen concentration,

† This work was supported in part by National Institutes of Health Grants HL-17655, HL-38324, and HL-53860 (to C.J.C.H.) and Established Investigator Award (to J.L.Z.) and Grant-in-Aid (to P.K.) from the American Heart Association.

* Author to whom correspondence should be addressed.

‡ C.J.C.H. dedicates the development of PNA to the memory of the late Professor Lawrence H. Piette.

⊗ Abstract published in *Advance ACS Abstracts,* April 15, 1996.

[1] Abbreviations: EPR, electron paramagnetic resonance; TPL, 4-hydroxy-2,2,6,6-tetramethylpiperidine-1-oxyl; TPH, 4-hydroxy-2,2,6,6-tetramethylpiperidine-1-hydroxyl; HSA, human serum albumin; PNA, polynitroxyl-albumin; MRI, magnetic resonance imaging; EPRI, electron paramagnetic resonance imaging; 3D, three dimensional.

S0006-2960(95)02857-1 CCC: $12.00

membrane permeability, extracellular reduction by ascorbate, and possible reoxidation of the reduced form by nitroxide (Chen & Swartz, 1988; Iannone et al., 1989; Nettleton et al., 1988). Thus the decay of the nitroxide *in vivo* is a complex process, requiring a thorough assessment of all these factors. In the present study, results are presented which demonstrate that novel polynitroxylated human serum albumin (PNA) when used with 4-hydroxy-2,2,6,6-tetramethylpiperidine-1-oxyl (TEMPOL or TPL) is capable of reoxidizing the reduced hydroxylamine 4-hydroxy-2,2,6,6-tetramethylpiperidine-1-hydroxyl (TPH) in the ischemic heart tissue and thus maintaining the EPR signal intensity of TPL. This enabled high-resolution EPR images of the heart to be acquired for prolonged periods during the development of global cardiac ischemia. Potential therapeutic applications of nitroxides used in conjunction with PNA in the treatment of free radical-mediated diseases are discussed.

MATERIALS AND METHODS

Preparation of PNA. PNA was prepared by allowing human serum albumin (HSA) to react with 60 molar equiv of 4-(2-bromoacetamido)-TEMPO (Br-TEMPO) at 60 °C for 10 h with mixing. The resulting mixture was sterilized with a 0.22 μm filter and transferred to a stirred filtration cell equipped with a 10 kDa cutoff membrane. The reaction mixture was washed with Ringer's lactate solution until the filtrate contained less than 1 μM free TEMPO as detected by ESR spectroscopy. The bright orange-colored retentate was then concentrated to 20% HSA, sterile filtered, and stored at 4 °C until use. The molar ratio of nitroxyl residues per mol of albumin was calculated from the spin density of polynitroxyl-albumin, measured by double integration of the EPR spectrum, calibrated against standards.

Chemicals. HSA was purchased from Baxter Healthcare, Glendale, CA. The nitroxide, 4-hydroxy-2,2,6,6-tetramethylpiperidine-1-oxyl (^{14}N-TPL), was purchased from Sigma Chemical Co. (St. Louis, MO). The nitroxide ^{15}N-TPL (4-hydroxy-2,2,6,6-tetramethylpiperidine-d_{17}-^{15}N-oxyl) was purchased from CDN Isotopes (Quebec, Canada). All other chemicals used in the heart perfusion solution were obtained from standard sources. Deionized distilled water was used throughout.

EPR Spectroscopy and Imaging. EPR spectra were recorded using a custom-built L-band bridge (Zweier & Kuppusamy, 1988) and a ceramic three-loop, two-gap reentrant resonator (Chzhan et al., 1993). The details of the L-band EPR spectrometer, magnet, gradient coil assembly, and software used for data acquisition, analysis, and image reconstruction are described elsewhere (Kuppusamy et al., 1994, 1995a−c). Data acquisition and subsequent image reconstruction were performed using a personal computer (Gateway 2000, P5-60 MHz) as described previously (Kuppusamy et al., 1994, 1995c). The EPR kinetic experiments were performed using a special version of data acquisition software that was capable of performing fully automated data acquisition, baseline setting, integration of a selected segment, and quantitation as a function of time. The kinetic data were obtained by measuring the low-field line of the nitroxide spectrum (sweep width, 10.0 G) followed by double integration. Other spectroscopic data collection parameters were as follows: modulation amplitude, 0.15 G; time constant, 20 ms; scan time, 10 s; modulation frequency, 100 kHz; microwave power, 15 mW; microwave frequency, 1.20 GHz; temperature, 26 ± 1 °C.

Isolated Rat Heart Preparation. Female Sprague-Dawley rat hearts were prepared as described (Zweier & Kuppusamy, 1988; Kuppusamy et al., 1994), according to the method of Langendorf (1895). A fluid-filled latex balloon was inserted into the left ventricular cavity via the mitral opening. The heart was perfused retrogradely under a constant perfusion pressure of 80 mmHg with a modified Krebs bicarbonate perfusate bubbled with 95% O_2 and 5% CO_2. The temperature of the heart was maintained at 37 ± 1 °C. After 15 min of control perfusion, the perfusate flow was stopped and 3 mL of 2 mM TPL in perfusate with or without PNA was infused through a side arm close to the aortic cannula. The end of the nitroxide infusion was marked as the time of onset of ischemia. The heart was immediately transferred to a 16 mm EPR tube and placed in the resonator, and data acquisition was started immediately. About 3−5 min was required before the start of the first acquisition. The acquisition software was then programmed to perform automated kinetic measurements or projection acquisitions for imaging.

RESULTS

Oxidation of TPH to TPL in Vitro by PNA. The PNA used in this study contained 42 mol of piperidinyl nitroxide/mol of HSA. It was prepared as a stock solution with a HSA concentration of 5 g/dL in lactated Ringer's buffer and made a clear golden solution. Oxidation of TPH to TPL by PNA was demonstrated by monitoring the rate of appearance of the EPR signal of TPL in a rapid-mixing experiment. When equal volumes of PNA and 1 mM TPH were mixed at room temperature, the rate of conversion of TPH to TPL had a half-time of 5 s. All 42 mol of nitroxide on the PNA was capable of participating in this reaction. Thus, both the rate and magnitude of TPH oxidation by PNA were higher as would be expected if all the 42 equiv of the HSA-bound nitroxide moieties participated in the reaction.

Spectral Distinction of the EPR Signals of TPL and PNA. The nitroxide molecules which serve as the redox center of PNA are covalently attached to the albumin. In order to distinguish the free TPL signal unambiguously from signal originating in albumin-bound nitroxyl residues, this study used free ^{15}N-TPL and PNA prepared with ^{14}N-TEMPO. Figure 1 shows the EPR spectra of ^{15}N-TPL in lactated Ringer's solution and ^{14}N-PNA in the heart perfusate solution. Both solutions contained the equivalent of 4.5 g of HSA/100 mL. Perdeuterated ^{15}N-TPL (^{15}N, $I = {}^1/_2$) gives rise to a doublet spectrum in which the two peaks are separated by 24.0 G (Figure 1A). In contrast, PNA exhibits a broad, asymmetric triplet spectrum (Figure 1B). There is negligible PNA signal at the field strength where the low-field ($m_I = +{}^1/_2$) peak of the ^{15}N-TPL spectrum is located, so that this peak is a measure only of ^{15}N-TPL signal. Conversely, there is negligible ^{15}N-TPL signal at the field strength where the central PNA ($m_I = 0$) peak is located, so that this peak reflects only PNA concentration. Thus, ^{15}N-TPL and PNA can be quantitated individually in composite spectra. ^{15}N-TPL was therefore used throughout the EPR pharmacokinetic studies described here. However, it was important to demonstrate that ^{15}N-TPL was equivalent to ^{14}N-TPL in terms of bioreduction. In the absence of PNA, ^{14}N-

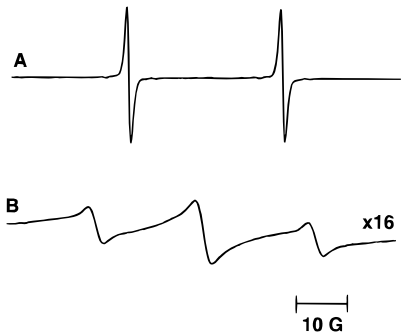

FIGURE 1: EPR spectra of (A) ^{15}N-TPL, 0.5 mL of 0.5 mM solution containing 5% human serum albumin, and (B) 0.5 mL of PNA in Ringer's lactate buffer. The concentrations correspond to those used in the heart experiments. Spectrum B, which is displayed at 16-fold higher gain relative to spectrum A, is asymmetrically broadened due to immobilization of the nitroxide residues bound to albumin. The instrumental settings were as follows: modulation field, 0.20 G; time constant, 20 ms; scan time, 10 s; modulation frequency, 100 kHz; microwave power, 15 mW; microwave frequency, 1.20902 GHz.

TPL and ^{15}N-TPL were indistinguishable in terms of their respective rates of reduction to the diamagnetic TPH (data not shown).

Reoxidation of TPH by PNA. Figure 2A shows the regeneration of TPL from TPH by PNA in the ischemic heart. TPL alone was first infused into the heart followed by global ischemia. The TPL signal was monitored for 30 min, during which time it decayed essentially to baseline. The first-order reduction rate constant of TPL was 0.20 ± 0.03 min^{-1}**.** This reduction rate corresponds with a half-life of 2.8 min. The loss of nitroxide signal intensity has been attributed to the rapid intracellular reduction of TPL to TPH (Swartz, 1987). To demonstrate that PNA is capable of reoxidizing TPH in the ischemic heart, the following experiment was performed: at the end of 30 min of global ischemia, when TPL had been completely reduced to TPH, 1 mL of PNA was infused into the heart and EPR spectra were recorded at 10 s intervals for the next 60 min. As shown in Figure 2A, the TPL signal reappeared and reached a maximum intensity within 2 min, followed by gradual decay.

The reappearance of the TPL signal is attributable to the transfer of an electron from TPH to PNA. The maximum TPL signal intensity was approximately 40% of the original TPL present in the heart (compare the initial signal intensity of segment II with that of segment I in Figure 2A). We attribute this to the washout of TPH in the vascular compartment by the infusion of PNA. The signal intensity decay curve was fitted with a sum of two first-order exponential functions with rate constants $k_1 = 0.08 \pm 0.03$ min^{-1} (50%) and $k_2 = 0.01 \pm 0.05$ min^{-1} (50%). The fast rate (k_1) has decreased by half (compare k_1 of segment I and segment II). The fast reduction rate (k_1) is attributable to the intracellular reduction of the TPL, while the slow reduction rate (k_2) is attributable to the decay of the fraction of the TPL whose intracellular reduction rate is moderated by its reoxidation in the extracellular space by PNA. These results clearly demonstrate that PNA reoxidizes bioreduced TPL in the ischemic heart.

Maintenance of TPL Signal in the Ischemic Heart by PNA. Figure 2B shows the TPL decay curves in the absence and presence of PNA measured in two different hearts. In the first heart the decay of TPL in the absence of PNA was monitored. The rate of reduction ($k = 0.24 \pm 0.03$ min^{-1}) was found to be similar to that shown in Figure 2A. However, in the second heart, which was infused with a mixture of PNA and TPL, the TPL signal in the ischemic heart was maintained for more than 2 h. The TPL decay curve appeared to be biphasic. The fast phase, with a rate constant of 0.21 ± 0.01 min^{-1} (70%), was similar to that of TPL in the absence of PNA. It is noteworthy that 70% of

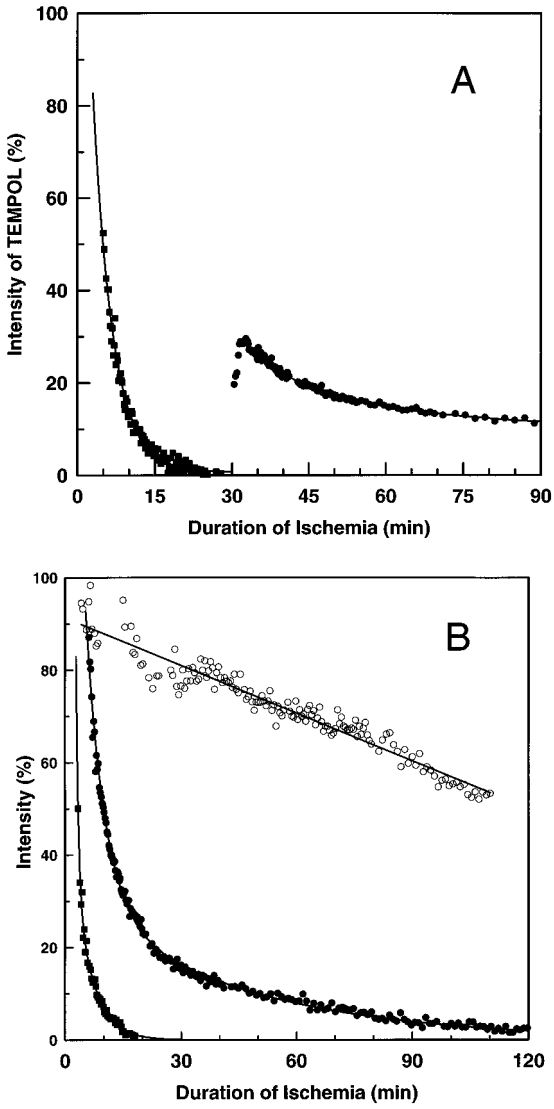

FIGURE 2: Decay and regeneration of ^{15}N-TPL. (A) Regeneration of ^{15}N-TPL from its reduced form in the ischemic rat heart by PNA. The reduction of the ^{15}N-TPL (■) was monitored for 30 min under global ischemia. At 30 min 1 mL of PNA solution was infused into the heart, and the measurements of the recovery of the ^{15}N-TPL signal (●) were continued for the next 60 min. The EPR signal intensity was normalized to 100% at the beginning of the experiment. The solid lines through the data points are fittings using a single exponential or sum of two exponentials, with rate constants of 0.20 min^{-1} (r^2, 0.986) for the 0−30 min segment and 0.08 and 0.01 min^{-1} (r^2, 0.991) for the 30−90 min segment. (B) Decay of ^{15}N-TPL (2 mM) alone (■), ^{15}N-TPL + PNA (●), and PNA alone (○) in the ischemic rat heart. Hearts were loaded with the test solution, placed inside the resonator, and then subjected to global ischemia. The peak intensities were individually normalized to 100% at the start of the measurements. The solid lines through the respective set of points are fittings using a single exponential or sum of two exponentials, with rate constants of 0.24 min^{-1} (r^2, 0.987) for ^{15}N-TPL and 0.21 and 0.023 min^{-1} (r^2, 0.996) for ^{15}N-TPL + PNA.

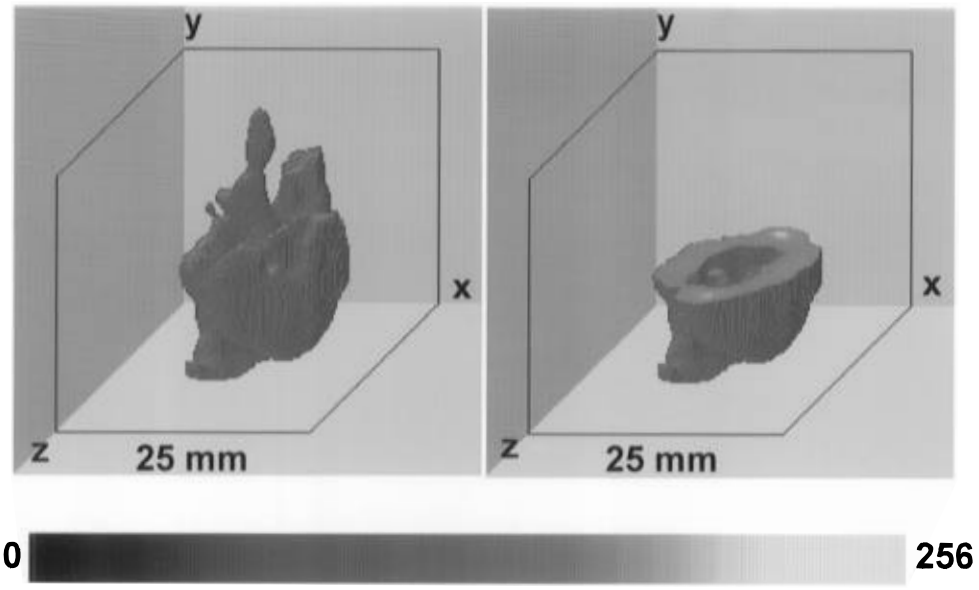

FIGURE 3: Three-dimensional (3D) spatial image of a rat heart loaded with ^{15}N-TPL and PNA and subjected to global ischemia. The left panel is a full view of the heart, and the right panel is a transverse cutout view of the heart. The left ventricular cavity in the center and the unpaired electron density contour of the heart are shown in the cutout view. The 3D spatial image was obtained from 144 projections acquired after ~2.5 h of ischemia. The measured projections were normalized for constant nitroxide intensity using the decay curve of Figure 2B and reconstructed by the filtered back-projection method on a 64 × 64 × 64 grid of integer array. Total acquisition time, 18 min; gradient, 20.0 G/cm.

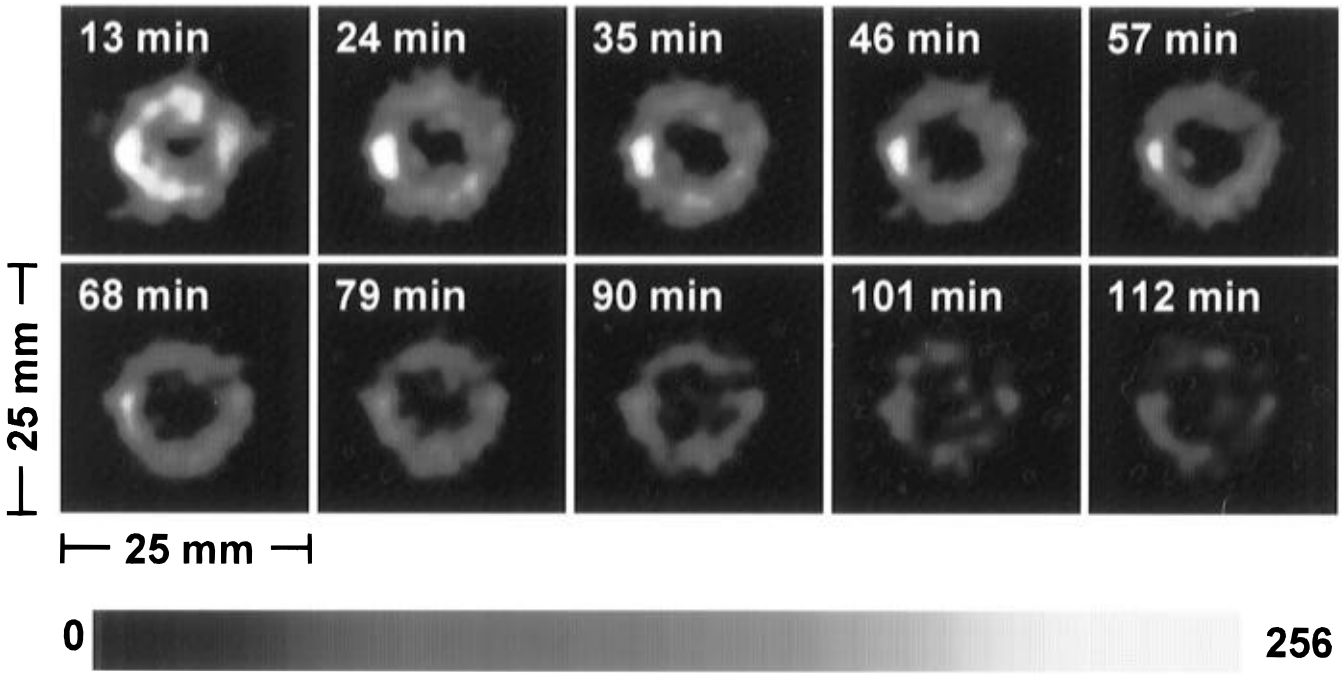

FIGURE 4: A series of 25 × 25 mm^2 transverse slices (thickness ~1 mm) of the isolated rat heart as a function of global cardiac ischemia. The transverse images of the heart reveal the presence of the left ventricular cavity and the TPL density maps as a function of time. The slices were obtained from the respective three-dimensional spatial images of a rat heart loaded with ^{15}N-TPL and PNA as in Figure 3. A series of 10 images were obtained each with 100 projections (acquisition time, 11 min) and 20.0 G/cm gradient. The mean value of the duration of ischemia (minutes) is marked on each slice.

the nitroxide was reduced at this rate. The slow phase (k_2), with a rate constant of 0.023 ± 0.002 min^{-1} (30%), was a result of the difference between the rate of reoxidation of TPH by PNA and that of k_1. The fraction of the TPL reduced during the slow phase is approximately 30%, as compared to that of 50% when the PNA was added after 30 min of ischemia. This difference appears to be attributable to the metabolic changes induced in the heart by ischemia, resulting in a decreased rate of TPL bioreduction.

3D Spatial EPR Imaging of the Ischemic Heart. Figure 3 shows a 3D spatial EPR image of TPL in the ischemic rat heart. The 3D image was reconstructed from 144 projections of the TPL signal, acquired 150 min after the onset of global cardiac ischemia. The cutout view of the heart shows the anatomic distribution of TPL in the heart. The left ventricular cavity, which was filled with an inflated balloon (~0.2 mL volume) is shown in the center. A relatively high concentration of TPL in the vascular space can be seen in the cutout view, where the aorta and right and left main coronary arteries appear as bright spots.

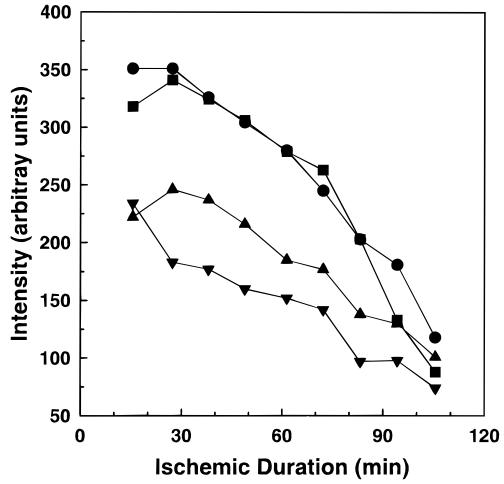

FIGURE 5: Plot of ^{15}N-TPL intensity at selected positions of the heart as a function ischemic duration: LAD (●), aortic (■), the tissue between the LAD and aortic blood vessels (▼), and LV apex (▲).

Changes in TPL Distribution in the Heart during Ischemia. Figure 4 shows a series of images of a 1 mm thick cross-sectional slice of the heart, acquired at 11-min intervals during 2 h of global ischemia. One hundred projections were acquired for each image and back-projected. A single short-axis cross-sectional slice of the heart from each of the 3D spatial images obtained during cardiac ischemia is presented. The overall decrease in TPL intensities in the presence of PNA is similar to that of TPL as shown in Figure 2B. The balloon-filled left ventricular cavity can be seen in the center of the slice.

Spatial Distribution of TPL: Intra- and Extravascular Concentrations. The unpaired electron density map of the heart shows distinct contours and signal decay rates as a function of time and location in the ischemic heart. Figure 5 shows the difference in nitroxide concentrations in the vascular space vs myocardium. The heart was positioned in the EPR cavity so that the left anterior descending artery (LAD) was at 9 o'clock and the aorta at 12 o'clock in the image. The relative signal intensities and rates of signal decay in LAD, the aorta, and the myocardium between these vessels and in the LV apex region are compared in Figure 5. Near the onset of ischemia, TPL concentration in the blood vessels is approximately 1.5 times that in myocardium. These differential intensities begin to converge approximately 2 h after the onset of global ischemia. However, even after 2.5 h of ischemia, anatomical differences in TPL signal intensity can still be clearly seen in the cutout view shown in Figure 3.

DISCUSSION

By virtue of their unpaired nitroxyl electron, nitroxides are paramagnetic probes whose EPR signal can provide metabolic information in biological systems, including information regarding tissue oxygenation and tissue redox state (Swartz, 1987; Swartz et al., 1986). Because of their paramagnetism, nitroxides decrease the relaxation times of hydrogen nuclei, and their usefulness as contrast agents in proton magnetic resonance imaging has been explored (Brasch, 1983; Brasch et al., 1983; Chan et al., 1990; Eriksson et al., 1988; Swartz, 1987). In general, nitroxides can add functional information to the considerable morphological data already available from MRI. Contrast enhancement obtained from nitroxides can augment and improve the diagnostic potential of MRI by differentiating isointense, but histologically dissimilar, tissues and by facilitating the localization and characterization of lesions such as blood brain barrier damage, abscesses, and tumors. Using doses of 1.0−2.5 mmol/kg, increases in spin echo intensities greater than 100% above baseline have been observed. Even at a nitroxide dose of 0.1 mmol/kg, the enhancing effect was easily detectable (Grodd et al., 1987). However, pharmacokinetic and metabolic studies of nitroxides indicate that they are rapidly reduced *in vivo* to diamagnetic, EPR-silent species, notably the hydroxylamine. This susceptibility of nitroxides to *in vivo* reduction has hindered the development of MRI applications. The ability of PNA to regenerate and sustain nitroxide levels in the ischemic heart opens the way to a renewed investigation of nitroxide as a nonionic MRI contrasting agent. EPR imaging using nitroxides as contrast agents also has the potential to add metabolic information to the structural information now obtained in proton MRI. Instrumentation for nitroxide EPR spectroscopy has been developed, but in previous studies signal duration and image quality have been limited by the short half-life of nitroxide *in vivo* (Zweier & Kuppusamy, 1988; Kuppusamy et al., 1994). This reduction has, until now, been irreversible *in vivo*. The present report introduces PNA, a novel polynitroxylated human serum albumin which is capable of oxidizing the hydroxylamine *in vivo*, thereby shifting the TPL/TPH equilibrium in favor of TPL. This occurs via spin transfer from the TPH to the albumin-bound nitroxyl residues. This phenomenon makes it possible to maintain useful TPL signal intensity in tissue for a prolonged period of time, allowing EPR imaging with improved image quality and duration. In comparison to our recent EPR image obtained with nitroxide alone (Kuppusamy et al., 1994), the images obtained with TPL in the presence of PNA (see Figures 3 and 4) allow strikingly improved stability and resolution of the ischemic isolated rat heart.

Due to its macromolecular nature, PNA is membrane impermeable and distributes in the extracellular and, when injected intravenously, primarily in the vascular space. This is in contrast with TPL and TPH, which are readily membrane permeable and move readily between the extra- and intracellular spaces. The intracellular space is the major site of nitroxide reduction (Chen et al., 1988; Swartz et al., 1986). When PNA is present, the hydroxylamine which diffuses back into the extracellular space is oxidized by PNA to nitroxide. This mechanism is schematically illustrated in Figure 6. The site of nitroxide reduction, inside the cell, is spatially distinct from the site of nitroxide regeneration by PNA in the extracellular space. In previous EPR imaging of nitroxides in the heart, images with submillimeter resolutions have been obtained; however, there was no resolution of intravascular vs extravascular structures. The lack of vascular contrast in previously reported EPR images of the ischemic heart (Kuppusamy et al., 1994) can be attributed to rapid equilibration of the nitroxide between the intra- and extracellular (mainly the vascular) space. With EPR imaging in the presence of PNA, however, the vascular structures including aorta and coronary arteries could be clearly distinguished.

In order to abolish the concentration gradient between the two compartments, the diffusion rate of nitroxide/hydroxy-

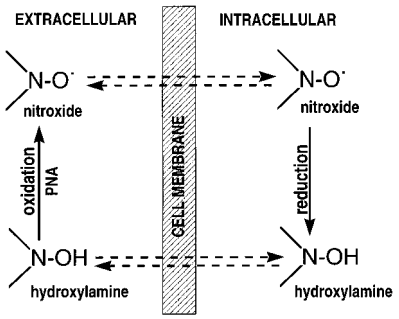

FIGURE 6: Schematic representation of the equilibrium of membrane-permeable nitroxide between the intra- and extracellular space and extracellular localization of PNA. The nitroxide is depicted to exist in its oxidized nitroxide state or reduced hydroxylamine state, both freely permeable to the cell membrane. PNA, being macromolecular in nature, is membrane impermeable and stays in the extracellular space. In the intracellular space, reduction converts the nitroxide molecule to its diamagnetic hydroxylamine derivative, resulting in a decrease in the EPR signal intensity. In the extracellular space the hydroxylamine is reoxidized to the nitroxide (paramagnetic) by PNA, thus regenerating the EPR signal.

lamine across the membrane has to be faster than the rate of intracellular nitroxide reduction. In order to maintain a concentration gradient of the nitroxide between the intra- and the extracellular spaces, the rate of oxidation of the reduced nitroxide by PNA has to be much faster than that of the equilibration of the nitroxide across the membrane barriers. These membrane diffusion barriers extend into the intracellular space where the volume defined by the mitochondria is believed to be the primary site of nitroxide reduction (Chen et al., 1988). The tissue or cellular nitroxide concentration is expected to decrease as its distance or number of membrane barriers increases from the vascular compartment. For example, the nitroxide concentration in the endothelium is expected to be higher than that of the smooth muscle, assuming similar intracellular nitroxide reduction rates. The slow phase of the nitroxide reduction in the presence of PNA represents the net difference between the cumulative intracellular reduction of all cells versus the extracellular (vascular) oxidation of the nitroxide by PNA. According to the hypothesis discussed in Figure 6, at the onset of global cardiac ischemia the extracellular, intracellular, and mitochondrial volume may be defined by the fraction of nitroxide reduced at different rate constants. In the presence of PNA, the proportion of nitroxide reduced at the rate of k_1 is decreased to 70%. This volume represents the volume of the intracellular space, wherein the nitroxide is prevented from rapid equilibration with 30% of the extracellular and vascular volume occupied by PNA.

The change in fractional and rate constants of nitroxide after 30 min of global ischemia may reveal changes in cellular redox state and fluid shift of the cardiac tissue. The reduction rates of TPL obtained from two different hearts are similar in the absence of PNA (Figure 2). However, the fraction and rate constants of the PNA regenerated TPL after 30 min of ischemia are different. Both k_1 and k_2 have been reduced for more than 50%. A shift of fluid compartment volume of the cardiac tissue is implied from the changes in the PNA reoxidation fraction of the TPL, increased from 30% to 50%. These data suggest that while only 30% of the TPL was in direct contact with the PNA at the onset of ischemia, after 30 min of ischemia this is increased to 50%. This increase is most likely due to myocardial cell death which is known to occur with ischemic duration greater than 30 min at 37 °C (Zweier, 1988; Shandelya et al., 1993).

The EPR signal of the 42 bound nitroxyl residues per albumin molecule gives rise to a spectrum in which the resonance peaks are considerably broadened (see Figure 1B). This is attributable to the combined effect of nitroxide immobilization and potential spin−spin (exchange and dipole) interactions between neighboring nitroxide moieties. Abolition of such spin−spin interactions would result in a sharp increase in resonance peak intensity due to narrowing of the line width. This effect has been previously used in a quantitative spin-membrane immunoassay (Hsia & Tan, 1978). In the present study, the reduction of nitroxide moieties on PNA in the process of TPH oxidation in the ischemic heart would reduce this proximity effect and result in a sharp increase in signal intensity. However, this spectral change did not occur. Rather, the resonance peak intensity decreased linearly throughout the 2 h global cardiac ischemia (see Figure 2B). The peak broadening observed with PNA is therefore consistent with the interpretation that motional immobilization is the major contributing factor to the observed resonance peak broadening of the nitroxide. The lack of spectral line overlap of TPL and PNA shown in this study makes possible distinct and quantitative kinetic and imaging measurement of these two compounds.

In the present work, the maintenance of nitroxide levels by PNA has been studied focusing on the utility of the nitroxide EPR spectrum as a tool for biomedical imaging of tissue metabolism. The results reported here clearly demonstrate that PNA is capable of reoxidizing bioreduced nitroxide under physiological conditions, although we have not yet precisely defined the reaction mechanism(s). Nitroxides have been shown by a number of laboratories to function as antioxidant enzyme mimics, with potential utility in the treatment of the wide range of diseases where injury is mediated by toxic (reduced) oxygen species. These include ischemia−reperfusion injury**,** inflammation, and injury by ionizing radiation. The demonstration of efficient reoxidation of reduced nitroxide by PNA means that the potentially important therapeutic (Gelvan et al., 1991; Hahn et al., 1994; Johnstone et al., 1995; Mehlhorn & Swanson, 1992; Reddan et al., 1993; Voest et al., 1993) and diagnostic (Brasch, 1983; Brasch et al., 1983; Eriksson et al., 1988) applications of nitroxides, which have until now been frustrated by the rapid bioreduction of nitroxide, may now be reevaluated.

REFERENCES

Berliner, L. J. (1992) Applications of EPR Imaging to Materials, Agriculture and Medicine, in *Magnetic Resonance Microscopy* Blumich, B., & Kuhn, W., Eds.) pp 151−163, VCH Publishers, Weinheim, Germany.

Berliner, L. J., Fujii, H., Wan, X., & Lukiewicz, S. J. (1987) *Magn. Reson. Med. 4*, 380−384.

Brasch, R. C. (1983) *Radiology 147*, 781−788.

Brasch, R. C., London, D. A., Wesbey, G. E., Tozer, T., Nitecki, D., Williams, R., Doemeny, J., Tuck, L., & Lallemand, D. (1983) *Radiology 147*, 773−779.

Chan, H.-C., Sun, K., Magin, R. L., & Swartz, H. M. (1990) *Bioconjugate Chem. 1*, 32−36.

Chen, K., & Swartz, H. M. (1988) *Biochim. Biophys. Acta 970*, 270−277.

Chen, K., Morse, P. D., II, & Swartz, H. M. (1988) *Biochim. Biophys. Acta 943*, 477−484.

Chzhan, M., Shteynbuk, M., Kuppusamy, P., & Zweier, J. L. (1993) *J. Magn. Reson. A105*, 49−53.
Eriksson, U. G., Schuhmann, G., Brasch, R. C., & Tozer, T. N. (1988) *J. Pharm. Sci. 77*, 97−103.
Gelvan, G., Saltman, P., & Powell, S. R. (1991) Proc. Natl. Acad. Sci. U.S.A. *88*, 4580−4684.
Grodd, W., Paajanen, H., Eriksson, U. G., Revel, D., Terrier, F., & Brasch, R. C. (1987) *Acta Radiol. 28*, 593−600.
Hahn, S. M., Krishna, C. M., Samuni, A., DeGraff, W., Cuscela, D. O., Johnstone, C., & Mitchell, J. B. (1994) *Cancer Res. (Suppl.) 54*, 2006s−2010s.
Hsia, J. C., & Tan, C. T. (1978) *Ann. N.Y. Acad. Sci. 308*, 139−148.
Iannone, A., Bini, A., Swartz, H. M., Tomasi, A., & Vannini, V. (1989) *Biochem. Pharmacol. 38*, 2581−2586.
Johnstone, P. A. S., DeGraff, W. G., & Mitchell, J. B. (1995) *Cancer 75*, 2323−2327.
Krishna, C. M., Grahame, D. A., Samuni, A., Mitchell, J. B., & Russo, A. (1992) *Proc. Natl. Acad. Sci. U.S.A. 89*, 5537−5541.
Kuppusamy, P., Chzhan, M., Vij, K., Shteynbuk, M., Lefer, D. J., Giannella, E., & Zweier, J. L. (1994) *Proc. Natl. Acad. Sci. U.S.A. 91*, 3388−3392.
Kuppusamy, P., Chzhan, P., & Zweier, J. L. (1995a) *J. Magn. Reson. B106*, 122−130.
Kuppusamy, P., Chzhan, M., Samouilov, A., Wang, P., & Zweier, J. L. (1995b) *J. Magn. Reson.* B *107*, 116−125.
Kuppusamy, P., Wang, P., & Zweier, J. L. (1995c) *Magn. Reson. Med. 34*, 99−105.
Langendorf, O. (1895) *Pfluegers Arch. Gesamte Physiol. Menschen Tiere 61*, 291−332.
Martinez-Yamout, M., & McConnell, H. M. (1994) *J. Mol. Biol. 244*, 301−318.
Mehlhorn, R. J., & Swanson, C. E. (1992) *Free Radical Res. Commun. 17*, 157−175.
Nettleton, D. O., Morse, P. D, II, & Swartz H. M. (1989) *Arch. Biochem. Biophys. 271*, 411−423.
Reddan, J. R., Sevilla, M. D., Gibli, F. J., Padgoankar, V., Dziedzic, D. C., Leverenz, V., Misra, I. C., & Peters, J. L. (1993) *Exp. Eye Res. 56*, 543−554.
Samuni, A., Krishna, C. M., Riesz, P., Finkelstein, E., & Russo, A. (1988) *J. Biol. Chem. 263*, 17921−17924.
Shandelya, S. M. L., Kuppusamy, P., Weisfeldt, M. L., & Zweier, J. L. (1993) *Circulation 87*, 536−546.
Swartz, H. M. (1987) *J. Chem. Soc., Faraday Trans. 83*, 191−202.
Swartz, H. M. (1989) in *Advances in Magnetic Resonance Imaging* (Feig, E., Ed.) pp 49−71, Ablex Publishing Co., Norwood, NJ.
Swartz, H. M., Sentjurc, M., & Morse, P. D., II (1986) *Biochim. Biophys. Acta 888*, 82−90.
Voest, E. E., van Faassen, E., & Marx, J. J. (1993) *Free Radical Biol. Med. 15*, 589−595.
Zweier, J. L. (1988) *J. Biol. Chem. 263*, 1353−1357.
Zweier, J. L., & Kuppusamy, P. (1988) *Proc. Natl. Acad. Sci. U.S.A. 85*, 5703−5707.

BI952857S